Contents lists available at ScienceDirect

Chemical Engineering Research and Design

journal homepage: www.elsevier.com/locate/cherd

Optimizing process economics and operational safety via economic MPC using barrier functions and recurrent neural network models

Zhe Wu[a], *Panagiotis D. Christofides*[a,b,*]

[a] *Department of Chemical and Biomolecular Engineering, University of California, Los Angeles, CA 90095-1592, USA*
[b] *Department of Electrical and Computer Engineering, University of California, Los Angeles, CA 90095-1592, USA*

ARTICLE INFO

Article history:
Received 18 September 2019
Received in revised form 9 October 2019
Accepted 11 October 2019
Available online 19 October 2019

Keywords:
Process safety
Control Lyapunov-barrier functions
Machine learning
Economic model predictive control
Nonlinear processes

ABSTRACT

In the present work, a control Lyapunov-barrier function (CLBF)-based economic model predictive control (EMPC) system is designed to optimize process economics, and ensure stability and operational safety simultaneously based on a prediction model using an ensemble of recurrent neural network (RNN) models. As accurate first-principles models are not available for many industrial processes, RNN models are utilized in this work to approximate the dynamics of a general class of nonlinear systems in an operating region. The ensemble of RNN models are incorporated in the design of CLBF-EMPC, under which guaranteed closed-loop stability and process operational safety are achieved for the nonlinear systems with two types of unsafe regions, i.e., bounded and unbounded sets. The application of the proposed RNN-based CLBF-EMPC method is demonstrated through a chemical process example with the case studies of a bounded and an of unbounded unsafe region, respectively.

1. Introduction

Safety is a major consideration in chemical process industries as the failure of safety-critical chemical systems may lead to severe consequences for both lives and property (Smith et al., 2003; Sanders, 2015). One novel perspective on process safety that has been advocated in several recent works (e.g., Leveson and Stephanopoulos, 2014; Venkatasubramanian, 2011; Mannan et al., 2015) is a systems view of process safety in which accidents are seen as the result of the process state migrating to an unsafe operating region from which an accident may quickly follow (like, for example, in the case of reactor thermal runaway). This is different from standard industrial thinking, which generally designs the systems that ensure operational safety of a chemical process via alarms on individual process components. To address the safety considerations regarding the avoidance of unsafe regions during operation, control barrier functions (CBF) (Wieland and Allgöwer, 2007; Tee et al., 2009; Niu and Zhao, 2013; Ames et al., 2019) that can enforce invariance of a level set of the barrier function due to its Lyapunov-like properties are utilized to maintain the process in a safe operating region for all times. Additionally, CBFs have been combined with control Lyapunov functions (CLF) via optimization-based method (Ames et al., 2014; Jankovic, 2017) (e.g., quadratic programming) or weighted average method (Romdlony and Jayawardhana, 2016) to simultaneously guarantee stability and safety. For example, in Romdlony and Jayawardhana (2016), control Lyapunov-barrier functions (CLBF) that are developed via the combination of independently designed CLFs and CBFs have been used to solve the problem of stabilization with guaranteed safety for nonlinear systems. Based on that, the integration of CLBFs in process control system designs that will allow the operation of safety-critical systems

* *Corresponding author at*: Department of Chemical and Biomolecular Engineering, University of California, Los Angeles, CA 90095-1592, USA.
E-mail address: pdc@seas.ucla.edu (P.D. Christofides).
https://doi.org/10.1016/j.cherd.2019.10.010

in a stable and safe manner has been demonstrated in Wu et al. (2019a).

Process economics is another important issue in chemical process industries due to increasing energy and material consumption. To attain higher economic profitability than the steady-state operation strategy, economic model predictive control (EMPC), a novel predictive control scheme formulated with an economic objective function is proposed to operate the system in a time-varying fashion (Heidarinejad et al., 2013; Angeli et al., 2012; Müller et al., 2013; Ellis et al., 2014). Though economic benefits are enhanced under EMPC, potential safety concerns may be brought up due to the possible extreme operating conditions in a chemical process (e.g., high temperature, pressure and flow rate in a chemical reactor) and EMPC systems addressing directly process operational safety should be designed. Motivated by these safety considerations, CLBF-based EMPC was proposed to address the tasks of simultaneous economic optimality, closed-loop stability and process operational safety. However, a key requirement for CLBF-based EMPC to achieve desired economic performance with guaranteed stability and safety is the availability of an accurate process model for the chemical process under control.

Modeling nonlinear processes has been extensively studied in the literature, within which, machine learning, a method of data analysis that help engineers learn from data and make decisions with minimal human intervention, has attracted an increasing attention and shown promising potential for modeling large-scale and complex nonlinear processes. Specifically, recurrent neural networks (RNN) have been utilized for modeling nonlinear dynamic systems using time-series data and have been demonstrated to be able to capture 'difficult nonlinearities' via a rich class of nonlinear functions (Kosmatopoulos et al., 1995; Ali et al., 2015; Wong et al., 2018). Additionally, a systematic method for incorporating RNNs in process control has been proposed in Wu et al. (2019c), in which RNN-based predictive controllers are designed to optimize process operational performance based on the prediction of process dynamics from RNN models. In this direction, machine learning techniques can be employed in CLBF-based EMPC to dynamically operate the system and improve closed-loop economic performance based on the predictions of RNN models.

Motivated by the above, in this work, we develop a machine-learning-based CLBF-EMPC that can handle stability, operational safety and closed-loop economic performance via CLBFs and RNN modeling techniques. The rest of the paper is organized as follows: in Section 2, we introduce the class of nonlinear systems considered, the recurrent neural network models, and the constrained control Lyapunov-barrier functions. In Section 3, a CLBF-based EMPC using an ensemble of RNN models is developed with provable feasibility, stability and safety accounting for bounded disturbances and bounded modeling errors between RNN models and the actual nonlinear process. In Section 4, the proposed RNN-based CLBF-EMPC is applied to a chemical process example with two case studies including a bounded and an unbounded unsafe region, to demonstrate its guaranteed operational safety.

2. Preliminaries

2.1. Notation

The Euclidean norm of a vector is denoted by the operator $|\cdot|$ and the weighted Euclidean norm of a vector is denoted by the operator $|\cdot|_Q$ where Q is a positive definite matrix. x^T denotes the transpose of x. The notation $L_fV(x)$ denotes the standard Lie derivative $L_fV(x) := \frac{\partial V(x)}{\partial x} f(x)$. A scalar continuous function $V : \mathbf{R}^n \to \mathbf{R}$ is proper if the set $\{x \in \mathbf{R}^n | V(x) \leq k\}$ is compact for all $k \in \mathbf{R}$, or equivalently, V is radially unbounded (Malisoff and Mazenc, 2009). For given positive real numbers β and ϵ, $\mathcal{B}_\beta(\epsilon) := \{x \in \mathbf{R}^n \,||\, x - \epsilon \,| < \beta\}$ is an open ball around ϵ with radius of β. The null set is denoted by $\emptyset$. Set subtraction is denoted by "\", i.e., $A \setminus B := \{x \in \mathbf{R}^n | x \in A, x \notin B\}$. A function $f(\cdot)$ is of class $\mathcal{C}^1$ if it is continuously differentiable. A continuous function $\alpha : [0, a) \to [0, \infty)$ is said to belong to class $\mathcal{K}$ if it is strictly increasing and is zero only when evaluated at zero.

2.2. Class of systems

We consider the class of continuous-time nonlinear systems with the following state-space form:

$$\dot{x} = F(x, u, w) := f(x) + g(x)u + h(x)w, \quad x(t_0) = x_0 \tag{1}$$

where $x \in \mathbf{R}^n$ is the state vector, $u \in \mathbf{R}^m$ is the manipulated input vector, and $w \in \mathbf{W}$ is the disturbance vector, where $\mathbf{W} := \{w \in \mathbf{R}^l \,||\, w\,| \leq \theta, \theta \geq 0\}$. The manipulated input vector is constrained by $u \in U := \{u_{\min} \leq u \leq u_{\max}\} \subset \mathbf{R}^m$, where u_{min} and u_{max} represent the minimum and the maximum value vectors of inputs allowed, respectively. $f(\cdot)$, $g(\cdot)$, and $h(\cdot)$ are sufficiently smooth vector and matrix functions of dimensions $n \times 1$, $n \times m$, and $n \times l$, respectively. Without loss of generality, the initial time t_0 is taken to be zero ($t_0 = 0$), and it is assumed that $f(0) = 0$ such that the origin is a steady-state of the system of Eq. (1) with $w(t) \equiv 0$.

A positive definite and proper control Lyapunov function (CLF) V is assumed to exist for the nominal system of Eq. (1) with $w(t) \equiv 0$ such that the small control property (i.e., for every $\varepsilon > 0$, $\exists \delta > 0$, s.t. $\forall x \in \mathcal{B}_\delta(0)$, there exists u that satisfies $|u| < \varepsilon$ and $L_fV(x) + L_gV(x)u < 0$, (Sontag, 1989)) and the following condition are satisfied:

$$L_fV(x) < 0, \quad \forall x \in \{z \in \mathbf{R}^n \setminus \{0\} \,|\, L_gV(z) = 0\} \tag{2}$$

Under the above assumption, a stabilizing feedback control law $\Phi(x) \in U$ that renders the origin of the closed-loop system asymptotically stable for all x in a neighborhood of the origin exists for the nominal system of Eq. (1) (i.e., $w(t) \equiv 0$) in the sense that Eq. (2) holds for $u = \Phi(x) \in U$.

2.3. Recurrent neural network model

A recurrent neural network (RNN) model that approximates the nonlinear dynamics of the system of Eq. (1) is developed with the following form:

$$\dot{\hat{x}} = F_{nn}(\hat{x}, u) := A\hat{x} + \Theta^T y \tag{3}$$

where $\hat{x} \in \mathbf{R}^n$ is the RNN state vector and $u \in \mathbf{R}^m$ is the manipulated input vector. $y = [y_1, \ldots, y_n, y_{n+1}, \ldots, y_{m+n}] = [\sigma(\hat{x}_1), \ldots, \sigma(\hat{x}_n), u_1, \ldots, u_m] \in \mathbf{R}^{n+m}$ is a vector of both the network state $\hat{x}$ and the input u, where $\sigma(\cdot)$ is the nonlinear activation function (e.g., a sigmoid function $\sigma(x) = 1/(1 + e^{-x})$). A is a diagonal coefficient matrix, i.e., $A = diag\{-a_1, \ldots, -a_n\} \in \mathbf{R}^{n \times n}$, where a_i is assumed to be positive such that each state $\hat{x}_i$ is bounded-input bounded-state stable. Θ is a weight matrix, i.e., $\Theta = [\theta_1, \ldots, \theta_n] \in \mathbf{R}^{(m+n) \times n}$ with $\theta_i = b_i[w_{i1}, \ldots, w_{i(m+n)}]$, $i = 1, \ldots, n$, where b_i is a constant and w_{ij} is the weight connecting

the jth input to the ith neuron where $i = 1, \ldots, n$ and $j = 1, \ldots, (m+n)$. Since the RNN model of Eq. (3) is an input-affine system, it can also be written in the form that is similar to Eq. (1):

$$\dot{x} = \hat{f}(x) + \hat{g}(x)u \tag{4}$$

where $\hat{f}(\cdot)$ and $\hat{g}(\cdot)$ can be derived from the coefficient matrices A and Θ in Eq. (3) and are assumed to be sufficiently smooth. During the training process of an RNN model, the modeling error between the RNN system of Eq. (3) and the nonlinear system of Eq. (1) is required to be bounded by $|\nu| = |F(x, u, 0) - F_{nn}(x, u)| \leq \gamma|x| \leq \nu_m$, where $\nu_m > 0$ is the upper bound of the modeling error ν within the operating region and $\gamma > 0$, such that the RNN model of Eq. (3) has the same steady-state as the nonlinear system of Eq. (1). Similarly, we assume that there exists a control Lyapunov function V and a stabilizing controller $u = \Phi_{nn}(x) \in U$ that renders the origin of the RNN system of Eq. (3) asymptotically stable in the sense that Eq. (2) (with $\hat{f}$ and $\hat{g}$ replacing f and g) is satisfied for the RNN system of Eq. (4) under $u = \Phi_{nn}(x) \in U$. Additionally, throughout the manuscript, we will use x and $\hat{x}$ to represent the state of the nonlinear system of Eq. (1) and of the RNN model of Eq. (3), respectively.

Remark 1. It is noted that in general, it is difficult to guarantee the boundedness of modeling error for all states in state-space. During the training process, the modeling error constraint is applied to both training dataset and validation training dataset that cover the initial conditions in the operating region as a stopping criterion of the training process. Therefore, the modeling error within the operating region can be regarded as being bounded after the training process is finished.

Remark 2. The dataset for training an RNN model generally come from the process data in industry, experiments, and simulations. In this work, we run extensive open-loop simulations with different combinations of initial conditions and control actions within the operating region to guarantee that the obtained RNN model can well represent the nonlinear process in this region. Additionally, we develop multiple RNN models based on a k-fold cross-validation. Specifically, the entire dataset is separated into k subsets and each time we use one of them as validation dataset and the remaining $k-1$ subsets as training datasets. Therefore, we derive k different RNN models for the same nonlinear process without having to increasing the amount of data samples.

2.4. *Stabilization and safety via control Lyapunov-barrier function-based control*

In Wu et al. (2019c), it has been demonstrated that the RNN-based controller $u = \Phi_{nn}(x) \in U$ is able to stabilize the nonlinear system of Eq. (1) at the origin provided that the RNN model is trained with a sufficiently small modeling error. Another important issue that remains to be investigated is process operational safety under the RNN-based controller. Specifically, it is noted that an unsafe region might exist for the operation of chemical processes based on the safety analysis either from first-principles models or process operational data. Generally, there are two types of unsafe regions: (1) unbounded sets, for example, an unsafe region consisting of all the states above a threshold that indicates an unsafe operation, and (2) bounded sets, which can be characterized based on multiple process states accounting for their interaction (e.g., a combination of temperature and concentration of reactants that reflect reaction rates in a chemical process example). Bounded unsafe sets are also commonly used in motion planning for robots and self-driving cars, which can be found in Mehra et al. (2015). In this work, we will address both bounded unsafe regions (denoted by $\mathcal{D}_b$) and unbounded unsafe regions (denoted by $\mathcal{D}_u$) and demonstrate that simultaneous closed-loop stability and process operational safety for the nonlinear system of Eq. (1) can be achieved under the RNN-based predictive controller.

Assuming that there exists a set of unsafe states $\mathcal{D} \subset \mathbf{R}^n$ in state-space, within which the operation of the system of Eq. (1) becomes unsafe, a feedback controller will be designed to achieve simultaneous closed-loop stability and process operational safety for the nonlinear system of Eq. (1) in the following sense:

Definition 1. Wu et al. (2019a)

Consider the system of Eq. (1) subject to the input constraints $u \in U$. If there exists a control law $u = \Phi(x) \in U$ such that for any initial state $x(t_0) = x_0$ in a safe stability region $\mathcal{U}$, where $\mathcal{U} \cap \mathcal{D} = \emptyset$ and $\{0\} \subset \mathcal{U}$, $x(t)$ remains inside $\mathcal{U}$, $\forall t \geq 0$, and the origin of the closed-loop system of Eq. (1) can be rendered asymptotically stable, we say that the control law $\Phi(x)$ maintains the process state within a safe stability region $\mathcal{U}$ at all times.

Based on a control Lyapunov function that satisfies the small control property and Eq. (2), and a control barrier function (CBF) that is designed to ensure boundedness of state in a safe operating region (see Wieland and Allgöwer, 2007), a constrained control Lyapunov-barrier function (CLBF) is developed in Romdlony and Jayawardhana (2016), Wu et al. (2019a) via the weighted average of a CLF and a CBF for the input-constrained nonlinear system of Eq. (1) to achieve process safety and stability simultaneously. The definition of a constrained CLBF is as follows:

Definition 2. Given a set of unsafe states in state-space $\mathcal{D}$, a proper, lower-bounded and $\mathcal{C}^1$ function $W_c(x) : \mathbf{R}^n \to \mathbf{R}$ is a constrained CLBF if $W_c(x)$ has a minimum at the origin and also satisfies the following properties:

$$W_c(x) > \rho, \quad \forall x \in \mathcal{D} \subset \phi_{uc} \tag{5a}$$

$$L_{\hat{f}} W_c(x) < 0, \quad \forall x \in \{z \in \phi_{uc} \backslash (\mathcal{D} \cup \{0\} \cup \mathcal{X}_e) \,|\, L_{\hat{g}} W_c(z) = 0\} \tag{5b}$$

$$\mathcal{U}_\rho := \{x \in \phi_{uc} \,|\, W_c(x) \leq \rho\} \neq \emptyset \tag{5c}$$

where $\rho \in \mathbf{R}$, and $\mathcal{X}_e := \{x \in \phi_{uc} \backslash (\mathcal{D} \cup \{0\}) \,|\, \partial W_c(x)/\partial x = 0\}$ is a set of stationary states (other than the origin) in state-space. It is noted that $\mathcal{X}_e$ is excluded in Eq. (5b) since $L_{\hat{f}} W_c(x)$ for the RNN model of Eq. (4) is rendered to be zero for $x \neq 0$ due to $\partial W_c(x)/\partial x = 0$, $\forall x \in \mathcal{X}_e$. The construction method of the constrained CLBF of Eq. (5) can be found in Romdlony and Jayawardhana (2016) and Wu et al. (2019a).

We assume that a feedback control law $u = \Phi_{nn}(x) \in U$ that renders the origin exponentially stable within an open neighborhood ϕ_{uc} that includes the origin in its interior exists for

the RNN system $\dot{x} = F_{nn}(x, u)$ (also in the form of Eq. (4), i.e., $\dot{x} = \hat{f}(x) + \hat{g}(x)u$) in the sense that there exists a $\mathcal{C}^1$ CLBF $W_c(x)$ that has a minimum at the origin and satisfies the following inequalities $\forall x \in \phi_{uc}$:

$$\hat{c}_1|x|^2 \leq W_c(x) - \rho_0 \leq \hat{c}_2|x|^2, \tag{6a}$$

$$\frac{\partial W_c(x)}{\partial x} F_{nn}(x, \Phi_{nn}(x)) \leq -\hat{c}_3|x|^2, \quad \forall x \in \phi_{uc} \backslash \mathcal{B}_\delta(x_e) \tag{6b}$$

$$\left| \frac{\partial W_c(x)}{\partial x} \right| \leq \hat{c}_4|x| \tag{6c}$$

where $\hat{c}_j(\cdot)$, $j = 1, 2, 3, 4$ are positive real numbers, $W_c(0) = \rho_0$ is the global minimum value of $W_c(x)$ in ϕ_{uc}, and $\mathcal{B}_\delta(x_e)$ is a small neighborhood around $x_e \in \mathcal{X}_e$. Due to the existence of a set of stationary points (for $x \neq 0$) in the presence of a bounded unsafe region (Braun and Kellett, 2018), $\frac{\partial W_c(x)}{\partial x}$ is close to zero in a neighborhood around the stationary point x_e, where $\frac{\partial W_c(x)}{\partial x} = 0$, and thus, Eq. (6b) does not hold for all $x \in \mathcal{B}_\delta(x_e)$. An example of the feedback control law $\Phi_{nn}(x)$ that satisfies the above conditions can be developed using the universal Sontag controller (Lin and Sontag, 1991) with $W_c(x)$ replacing the Lyapunov function $V(x)$ (Wu et al., 2019a). Additionally, by continuity and the smoothness assumed for f, g and h in the nonlinear system of Eq. (1), there exist positive constants M, L_x, L_w, L'_x, L'_w such that the following inequalities hold for all $x, x' \in \mathcal{U}_\rho$, $u \in U$, and $w \in W$:

$$|F(x, u, w)| \leq M \tag{7a}$$

$$|F(x, u, w) - F(x', u, 0)| \leq L_x|x - x'| + L_w|w| \tag{7b}$$

$$|\frac{\partial W_c(x)}{\partial x} F(x, u, w) - \frac{\partial W_c(x')}{\partial x} F(x', u, 0)| \leq L'_x|x - x'| + | \leq L'_w|w_m| \tag{7c}$$

The following theorem is established to demonstrate that closed-loop stability and process operational safety can be achieved simultaneously for the RNN system of Eq. (3) (also in the form of Eq. (4)) under the controller $u = \Phi_{nn}(x) \in U$. Similar analysis for the nonlinear system of Eq. (1) associated with bounded and unbounded unsafe regions can be found in Wu and Christofides (2019).

Theorem 1. *Consider the RNN system of Eq. (3) with a constrained CLBF $W_c(x)$ of Eq. (5) that has a minimum at the origin and the controller $u = \Phi_{nn}(x) \in U$ that satisfies Eq. (6). The state of the closed-loop system of Eq. (3) is guaranteed to be bounded in $\mathcal{U}_\rho$ for all times for any $x_0 \in \mathcal{U}_\rho$ under $u = \Phi_{nn}(x) \in U$. Additionally, the origin can be rendered exponentially stable under $u = \Phi_{nn}(x) \in U$ in the case of an unbounded unsafe region $\mathcal{D}_u$, while discontinuous control actions $u = \bar{u}(x) \in U$ (i.e., $\bar{u}(x) \neq \Phi_{nn}(x)$) that can drive the state in a direction of decreasing $W_c(x)$ are required for $x \in \mathcal{B}_\delta(x_e)$ in the presence of a bounded unsafe region $\mathcal{D}_b$.*

Proof. The boundedness of the state in the safe operating region $\mathcal{U}_\rho$ can be proven by showing that $\dot{W}_c \leq 0$, $\forall x \in \mathcal{U}_\rho$ holds for both bounded and unbounded unsafe regions under the controller $u = \Phi_{nn}(x) \in U$. In the presence of an unbounded unsafe region $\mathcal{D}_u$, exponential stability of the origin is derived under the continuous control actions $u = \Phi_{nn}(x) \in U$ since it has been demonstrated that in the absence of stationary points (for $x \neq 0$), i.e., $\mathcal{X}_e = \emptyset$, it holds that $\frac{\partial W_c(x)}{\partial x} F_{nn}(x, \Phi_{nn}(x)) \leq -\hat{c}_3|x|^2 < 0$, $\forall x \in \mathcal{U}_\rho \backslash \{0\}$ in Eq. (6b). However, considering that the origin is not the unique minimum in state-space in the presence of a bounded unsafe region $\mathcal{D}_b$, discontinuous control actions $u = \bar{u}(x) \in U$ are required to drive the state away from stationary points (i.e., $\mathcal{X}_e$) and towards the origin provided that the value of $W_c(x)$ decreases over time under $u = \bar{u}(x) \in U$. The detailed proof is omitted here as it is similar to those for Theorems 1 and 2 in Wu and Christofides (2019). □

3. CLBF-based EMPC using an ensemble of RNN models

In this section, an EMPC that incorporates RNN models and CLBF-based constraints will be developed to ensure closed-loop stability and process operational safety for the nonlinear system of Eq. (1). Specifically, we first present the formulation of Lyapunov-based EMPC that was proposed to derive closed-loop stability only for the nonlinear system of Eq. (1) (Heidarinejad et al., 2013). Additionally, a machine learning paradigm, termed ensemble learning, is introduced to combine multiple RNN models together to improve the prediction accuracy compared to a single RNN model. Subsequently, we present the formulation of the CLBF-EMPC and provide detailed stability and safety analysis for the nonlinear system of Eq. (1) under CLBF-EMPC.

3.1. *Lyapunov-based EMPC (LEMPC)*

The LEMPC design based on the RNN model of Eq. (3) is formulated as the following optimization problem:

$$\mathcal{J} = \max_{u \in S(\Delta)} \int_{t_k}^{t_{k+N}} l_e(\tilde{x}(t), u(t))dt \tag{8a}$$

$$\text{s.t.} \quad \dot{\tilde{x}}(t) = F_{nn}(\tilde{x}(t), u(t)) \tag{8b}$$

$$\tilde{x}(t_k) = x(t_k) \tag{8c}$$

$$u(t) \in U, \quad \forall t \in [t_k, t_{k+N}) \tag{8d}$$

$$V(\tilde{x}(t)) \leq \rho_e, \quad \forall t \in [t_k, t_{k+N}), \quad \text{if} \quad V(x(t_k)) \leq \rho_e \tag{8e}$$

$$\dot{V}(x(t_k), u(t_k)) \leq \dot{V}(x(t_k), \Phi_{nn}(t_k)) \quad \text{if} \quad V(x(t_k)) > \rho_e \tag{8f}$$

where $\tilde{x}(t)$ is the predicted state trajectory, $S(\Delta)$ is the set of piecewise constant functions with period Δ, and N is the number of sampling periods in the prediction horizon. The LEMPC is implemented in a sample-and-hold fashion, i.e., $u(t) = u(t_k)$, $\forall t \in [t_k, t_{k+1})$, where $t_{k+1} := t_k + \Delta$ and Δ is the sampling period. The economic objective function of Eq. (8a) is the time integral of $l_e(\tilde{x}(t), u(t))$ over the prediction horizon. The RNN model of Eq. (3) is utilized in Eq. (8b) to predict the states within the prediction horizon given the initial condition $x(t_k)$ and inputs $u(t)$, $\forall t \in [t_k, t_{k+N})$. The state measurement of Eq. (8c) at $t = t_k$ is taken as the initial condition for the prediction model of Eq. (8b). The input constraints of Eq. (8d) are applied over the entire prediction horizon. The LEMPC of Eq. (8) incorporates two Lyapunov-based constraints to maintain the state in Ω_ρ, which is a level set of Lyapunov function, i.e., $\Omega_\rho := \{x \in \mathbf{R}^n \mid V(x) \leq \rho, \rho > 0\}$. Specifically, under the constraint of Eq. (8e), the predicted state is required to be bounded in Ω_{ρ_e} if the current state $x(t_k) \in \Omega_{\rho_e}$, where $\rho_e < \rho$; however, under the constraint

of Eq. (8f), the state is forced to move towards the origin if $x(t_k)$ is in $\Omega_\rho \backslash \Omega_{\rho_e}$.

3.2. CLBF-based EMPC

Based on the RNN-based LEMPC of Eq. (8), an RNN-based CLBF-EMPC is developed in this section. Before we present the formulation of CLBF-EMPC, ensemble learning, a machine learning paradigm that combines multiple machine learning models to produce better predictions, is employed to improve RNN prediction performance. Specifically, we train k distinct RNN models for the same process, (i.e., the nonlinear system of Eq. (1)) using k-fold cross-validation to form an RNN ensemble, and then calculate the final prediction results by taking average of k RNN models. It is demonstrated in Wu et al. (2019c) that the overall prediction performance of an ensemble of multiple RNN models outperforms that of a single RNN model when implemented as the prediction model in MPC. Following the development method of multiple RNN models in the context of ensemble learning in Wu et al. (2019c), the CLBF-EMPC scheme using an ensemble of RNN models is represented by the following optimization problem:

$$\mathcal{J} = \max_{u \in S(\Delta)} \int_{t_k}^{t_{k+N}} L(\tilde{x}(t), u(t))dt \tag{9a}$$

$$\text{s.t.} \quad \dot{\tilde{x}}(t) = \frac{1}{N_e}\sum_{j=1}^{N_e} F_{nn}^j(\tilde{x}(t), u(t)) \tag{9b}$$

$$\tilde{x}(t_k) = x(t_k) \tag{9c}$$

$$u(t) \in U, \quad \forall t \in [t_k, t_{k+N}) \tag{9d}$$

$$W_c(\tilde{x}(t)) \le \rho_e, \quad \forall t \in [t_k, t_{k+N}), \quad \text{if} \quad W_c(x(t_k)) \le \rho_e \tag{9e}$$

$$\dot{W}_c(x(t_k), u(t_k)) \le \dot{W}_c(x(t_k), \Phi_{nn}(t_k)) \quad \text{if} \quad W_c(x(t_k)) > \rho_e \tag{9f}$$

where the notation follows that in Eq. (8) and the CLBF-EMPC is again implemented in a sample-and-hold fashion. Additionally, to simplify the notation, we use x instead of $\hat{x}$ to represent the RNN state in CLBF-EMPC since the optimization problem is merely based on the RNN model of Eq. (3). It is noted that instead of using a single RNN model, Eq. (9b) utilizes an ensemble of RNN models F_{nn}^j, $j = 1, \ldots, N_e$, where N_e is the total number of RNN models, to predict the evolution of states under a set of control actions. Similarly, two CLBF-based constraints are incorporated in the design of CLBF-EMPC to ensure boundedness of the state in the safe stability region $\mathcal{U}_\rho$ in Eq. (5). The constraint of Eq. (9e) is activated when the state $x(t_k)$ is in $\mathcal{U}_{\rho_e}$, where $\rho_e < \rho$. When the state leaves $\mathcal{U}_{\rho_e}$ due to disturbances or model mismatch (which will be discussed in the following section), the constraint of Eq. (9f) is applied to drive the state towards the origin. As a result, the state will move into $\mathcal{U}_{\rho_e}$ within finite sampling periods. Additionally, we assume that the state measurements of the closed-loop system of Eq. (1) is available at each sampling time. The CLBF-EMPC optimization problem of Eq. (9) will calculate an optimal input sequence $u^*(t)$, $\forall t \in [t_k, t_{k+N})$, but only the first control action of $u^*(t)$ will be applied over the next sampling period.

Before we establish the theorem to demonstrate simultaneous closed-loop stability and process operational safety for the nonlinear system of Eq. (1) under the RNN-based CLBF-EMPC of Eq. (9), the following proposition is developed to provide an upper bound for the error vector between the states of the nonlinear system of Eq. (1) and of the RNN system of Eq. (3).

Proposition 1. *Consider the nonlinear system $\dot{x} = F(x, u, w)$ of Eq. (1) subject to bounded disturbances $|w(t)| \le w_m$. If the modeling error is bounded, i.e., $|\nu| = |F(x, u, 0) - F_{nn}(x, u)| \le \gamma|x| \le \nu_m$, then there exists a class $\mathcal{K}$ function $f_w(\cdot)$ and a positive constant κ such that the following inequalities hold $\forall x, \hat{x} \in \mathcal{U}_\rho$ and $w(t) \in W$ with the same initial condition $x_0 = \hat{x}_0 \in \mathcal{U}_\rho$:*

$$|x(t) - \hat{x}(t)| \le f_w(t) := \frac{L_w w_m + \nu_m}{L_x}(e^{L_x t} - 1) \tag{10a}$$

$$W_c(x) \le W_c(\hat{x}) + f_e(|x - \hat{x}|) \tag{10b}$$

where

$$f_e(|x - \hat{x}|) := \frac{\hat{c}_4\sqrt{\rho - \rho_0}}{\sqrt{\hat{c}_1}}|x - \hat{x}| + \kappa|x - \hat{x}|^2 \tag{11}$$

Proof. The proof is omitted here due to space limitations. Interested readers may refer to the proof of Proposition 3 in Wu et al. (2019c). □

3.3. Stability and safety under CLBF-EMPC

Closed-loop stability and safety for the nonlinear system of Eq. (1) under the CLBF-EMPC of Eq. (9) will be proven in this section. It should be noted that for the operation of the nonlinear system of Eq. (1) under EMPC, the system is considered stable and safe if the state can be bounded in a safe stability region for all times for any initial condition inside of this region. In other words, the system is not required to be operated at the steady-state like what it is under tracking MPC since it is demonstrated that economic performance can be improved under time-varying operation than the steady-state operation.

The following proposition is developed to demonstrate that the feedback controller $u = \Phi_{nn}(x) \in U$ that maintains the state of the RNN model of Eq. (3) in the safe operating region $\mathcal{U}_\rho$ also ensures the boundedness of the state of the nonlinear system of Eq. (1) within $\mathcal{U}_\rho$ accounting for bounded disturbances (i.e., $|w(t)| \le w_m$), bounded modeling error (i.e., $|\nu| = |F(x, u, 0) - F_{nn}(x, u)| \le \gamma|x| \le \nu_m$) and sample-and-hold implementation of control actions.

Proposition 2. *Consider the system of Eq. (1) under the sample-and-hold implementation of the controller $u = \Phi_{nn}(x) \in U$ that meets the conditions of Eq. (6). If there exists a positive real number $\gamma < \hat{c}_3/\hat{c}_4$ such that for all $x \in \mathcal{U}_\rho$ and $u \in U$, the modeling error between the RNN model of Eq. (3) and the nonlinear system of Eq. (1) is constrained by $|\nu| = |F(x, u, 0) - F_{nn}(x, u)| \le \gamma|x|$, and there exist $\epsilon_w > 0$, $\Delta > 0$ and $\rho > \rho_e$ that satisfy*

$$-\frac{\tilde{c}_3}{\hat{c}_2}(\rho_e - \rho_0) + L_x' M\Delta + L_w' w_m \le -\epsilon_w \tag{12a}$$

$$\rho_e \le \rho - f_e(f_w(\Delta)) \tag{12b}$$

$$\mathcal{X}_e \subset \mathcal{U}_{\rho_e} \tag{12c}$$

where $f_w(t)$ and $f_e(t)$ are given by Eqs. (10a) and (11), respectively, then for any $x(t_k) \in \mathcal{U}_\rho$, the state of the nonlinear system of Eq. (1) is guaranteed to be bounded in $\mathcal{U}_\rho$ for all times.

Proof. We first prove that $\dot{W}_c(x)$ based on the state of the nonlinear system of Eq. (1) can be rendered negative under continuous implementation of $u = \Phi_{nn}(x) \in U$ for any $x \in \mathcal{U}_\rho \backslash \mathcal{U}_{\rho_e}$. The time-derivative of $W_c(x)$, $\forall x \in \mathcal{U}_\rho \backslash \mathcal{U}_{\rho_e}$ is derived as follows using Eqs. (6b) and (6c):

$$\begin{aligned}\dot{W}_c &= \frac{\partial W_c(x)}{\partial x} F(x, \Phi_{nn}(x), 0) \\ &= \frac{\partial W_c(x)}{\partial x}(F_{nn}(x, \Phi_{nn}(x)) + F(x, \Phi_{nn}(x), 0) - F_{nn}(x, \Phi_{nn}(x))) \\ &\le -\hat{c}_3|x|^2 + \hat{c}_4|x|(F(x, \Phi_{nn}(x), 0) - F_{nn}(x, \Phi_{nn}(x))) \\ &\le -\hat{c}_3|x|^2 + \hat{c}_4\gamma|x|^2\end{aligned} \tag{13}$$

Therefore, if γ is constrained by $\gamma < \hat{c}_3/\hat{c}_4$, it holds that $\dot{W}_c \le -\tilde{c}_3|x|^2 < 0$, $\forall x \in \mathcal{U}_\rho \backslash \mathcal{U}_{\rho_e}$ by letting $\tilde{c}_3 = -\hat{c}_3 + \hat{c}_4\gamma$. Next, we consider the impacts of bounded disturbances and of the sample-and-hold implementation of control actions (i.e., $u(t) = u(t_k)$, $\forall t \in [t_k, t_{k+1})$, where $t_{k+1} := t_k + \Delta$ and Δ is the sampling period) on closed-loop stability of the nonlinear system of Eq. (1). Assuming $x(t_k) = \hat{x}(t_k) \in \mathcal{U}_\rho \backslash \mathcal{U}_{\rho_s}$, the time-derivative of $W_c(x)$ in Eq. (13) for the nonlinear system of Eq. (1) subject to bounded disturbances (i.e., $|w| \le w_m$) can be derived as follows:

$$\begin{aligned}\dot{W}_c(x(t)) &= \frac{\partial W_c(x(t))}{\partial x} F(x(t), \Phi_{nn}(x(t_k)), w) \\ &= \frac{\partial W_c(x(t_k))}{\partial x} F(x(t_k), \Phi_{nn}(x(t_k)), 0) \\ &\quad + \frac{\partial W_c(x(t))}{\partial x} F(x(t), \Phi_{nn}(x(t_k)), w) \\ &\quad - \frac{\partial W_c(x(t_k))}{\partial x} F(x(t_k), \Phi_{nn}(x(t_k)), 0)\end{aligned} \tag{14}$$

Using Eq. (6b), Eq. (13) and the Lipschitz condition in Eq. (7), $\dot{W}_c(x(t))$ is bounded by the following inequality for all $t \in [t_k, t_{k+1})$ and $x(t_k) \in \mathcal{U}_\rho \backslash \mathcal{U}_{\rho_e}$:

$$\begin{aligned}\dot{W}_c(x(t)) &\le -\frac{\tilde{c}_3}{\hat{c}_2}(\rho_e - \rho_0) + \frac{\partial W_c(x(t))}{\partial x} F(x(t), \Phi_{nn}(x(t_k)), w) \\ &\quad - \frac{\partial W_c(x(t_k))}{\partial x} F(x(t_k), \Phi_{nn}(x(t_k)), 0) \\ &\le -\frac{\tilde{c}_3}{\hat{c}_2}(\rho_e - \rho_0) + L'_x|x(t) - x(t_k)| + L'_w|w| \\ &\le -\frac{\tilde{c}_3}{\hat{c}_2}(\rho_e - \rho_0) + L'_x M\Delta + L'_w w_m\end{aligned} \tag{15}$$

From Eq. (15), it is obtained that $\dot{W}_c(x(t)) \le -\epsilon_w$ holds for all $x(t_k) \in \mathcal{U}_\rho \backslash \mathcal{U}_{\rho_e}$ and $t \in [t_k, t_{k+1})$ if Eq. (12a) is satisfied.

So far we have demonstrated that for any state $x(t_k) \in \mathcal{U}_\rho \backslash \mathcal{U}_{\rho_e}$, the state does not leave $\mathcal{U}_\rho$ under the sample-and-hold implementation of $u = \Phi_{nn}(x) \in U$. It remains to show that for $x(t_k) \in \mathcal{U}_{\rho_e}$, the state of the nonlinear system of Eq. (1) will not leave $\mathcal{U}_\rho$ within one sampling period if the state predicted by the RNN system of Eq. (3) is bounded in $\mathcal{U}_{\rho_e}$. Specifically, for any $x(t_k) = \hat{x}(t_k) \in \mathcal{U}_{\rho_e}$, the following inequality is derived based on Eq. (10) and Eq. (11) for $t \in [t_k, t_{k+1})$:

$$\begin{aligned}W_c(x(t)) &\le W_c(\hat{x}(t)) + f_e(|x(t) - \hat{x}(t)|) \\ &\le W_c(\hat{x}(t)) + f_e(f_w(t - t_k)) \\ &\le \rho_e + f_e(f_w(\Delta))\end{aligned} \tag{16}$$

Therefore, if $\mathcal{U}_{\rho_e}$ is characterized to satisfy Eq. (12b), it follows that $W_c(x(t)) \le \rho$, which implies that the state of the nonlinear system of Eq. (1) is bounded in $\mathcal{U}_\rho$ within one sampling period. This completes the proof that the closed-loop state of the nonlinear system of Eq. (1) subject to bounded disturbances (i.e., $|w(t)| \le w_m$) is guaranteed to be bounded in the safe operating region $\mathcal{U}_\rho$ for any initial condition x_0 inside of this region under the sample-and-hold implementation of $u = \Phi_{nn}(x) \in U$. □

Remark 3. The issue of convergence to the stationary points (for $x \neq 0$) in the presence of a bounded unsafe region $\mathcal{D}_b$ is addressed by designing the set Ω_{ρ_e} to include the set of stationary points inside (i.e., Eq. (12c)). Specifically, since the state of the nonlinear system of Eq. (1) is not required to move towards the origin (or any stationary points) within Ω_{ρ_e} under the constraint of Eq. (9e), the state will not get stuck in a stationary point unless it is exactly the state where the objective function of CLBF-EMPC of Eq. (9) attains its maximum value. Therefore, the boundedness of the state in Ω_ρ is guaranteed for the nonlinear system of Eq. (1) with both bounded and unbounded unsafe regions when implementing $u = \Phi_{nn}(x) \in U$ in a sample-and-hold fashion. However, it should be noted that when the system is required to be operated at the steady-state under a tracking MPC, the stationary points need to be handled by a set of discontinuous control actions such that the state can escape from the stationary points and converge to the origin (Wu et al., 2019a; Wu and Christofides, 2019).

Based on Propositions 1 and 2, we establish the following theorem to demonstrate guaranteed closed-loop stability and process operational safety for the nonlinear system of Eq. (1) under the CLBF-EMPC of Eq. (9).

Theorem 2. *Consider the system of Eq. (1) with a CLBF W_c that satisfies Eq. (5). If there exist $\rho > \rho_e$ and $\gamma < \hat{c}_3/\hat{c}_4$ that satisfy the conditions in Propositions 1 and 2, then given any initial state $x_0 \in \mathcal{U}_\rho$, recursive feasibility of the CLBF-EMPC optimization problem of Eq. (9) and the boundedness of the state in the safe stability region $\mathcal{U}_\rho$ are guaranteed for all times.*

Proof. We first prove that a set of feasible solution exists for the CLBF-EMPC optimization problem of Eq. (9) for all states $x(t) \in \mathcal{U}_\rho$ by showing that the input trajectories $u(t) = \Phi_{nn}(x(t_{k+i})) \in U$, $\forall t \in [t_{k+i}, t_{k+i+1})$ with $i = 0, \ldots, N-1$ meet the constraints of the CLBF-EMPC optimization problem of Eq. (9). The discussion mainly focuses on the constraints of Eqs. (9e)–(9f) as the satisfaction of the input constraint $u \in U$ of Eq. (9d) is readily shown for the controller $u = \Phi_{nn}(x) \in U$. Specifically, if $x(t_k) \in \mathcal{U}_{\rho_e}$, the constraint of Eq. (9e) is satisfied under the sample-and-hold implementation of $u = \Phi_{nn}(x) \in U$ since the state of the RNN system of Eq. (3) will be steered towards the origin or the stationary points in the presence of a bounded unsafe region. In any case, the state is maintained in $\mathcal{U}_{\rho_e}$ under $u = \Phi_{nn}(x) \in U$. On the other hand, if $x(t_k) \in \mathcal{U}_\rho \backslash \mathcal{U}_{\rho_e}$, the set of control actions $u(t) = \Phi_{nn}(x(t_{k+i})) \in U$, $i = 0, \ldots, N-1$ is again a feasible solution that meets the constraints of Eq. (9f) (i.e.,

the inequality constraint of Eq. (9f) becomes an active constraint). This completes the proof of recursive feasibility for the CLBF-EMPC of Eq. (9).

The proof of the boundedness of the state in $\mathcal{U}_\rho$ follows the conclusions in Propositions 1 and 2. We first consider the case where $x(t_k) \in \mathcal{U}_{\rho_e}$. As it is required by the constraint of Eq. (9e) that the state $x(t)$, $\forall t \in [t_k, t_{k+1})$ predicted by the ensemble of RNN models of Eq. (9b) be bounded in $\mathcal{U}_{\rho_e}$, it follows from Eq. (16) that the state of the nonlinear system of Eq. (1) does not leave $\mathcal{U}_\rho$ within one sampling period. At the next sampling period, if $x(t_{k+1})$ remains in $\mathcal{U}_{\rho_e}$, it is again bounded in $\mathcal{U}_\rho$ following the above analysis. However, if $x(t_{k+1})$ enters $\mathcal{U}_\rho \backslash \mathcal{U}_{\rho_e}$, the constraint of Eq. (9e) is activated to drive the state of the RNN model of Eq. (3) towards the origin. Since it is proven in Proposition 2 that $\dot{W}_c$ based on the state of the nonlinear system of Eq. (1) can be rendered negative accounting for bounded disturbances and modeling error within one sampling period under $u = \Phi_{nn}(x) \in U$ (a feasible solution to the CLBF-EMPC optimization problem), the state of the nonlinear system of Eq. (1) is also able to move towards the origin and ultimately enters $\mathcal{U}_{\rho_e}$ within finite sampling periods. This completes the proof of closed-loop stability of the nonlinear system of Eq. (1) under CLBF-EMPC.

Additionally, since the safe stability region $\mathcal{U}_\rho$ does not intersect with the (bounded and unbounded) unsafe region (i.e., $\mathcal{U}_\rho \cap \mathcal{D} = \emptyset$) according to the definition of the constrained CLBF of Eq. (5), the state trajectory under the time-varying operation of the nonlinear system of Eq. (1) does not enter the unsafe region for all times. Therefore, process operational safety in terms of avoidance of the unsafe region is also guaranteed under CLBF-EMPC. □

Remark 4. It is noted that closed-loop stability and safety in Theorem 2 holds for the system of Eq. (1) subject to bounded disturbances (i.e., $|w(t)| \leq w_m$) as the effects of disturbances have been accounted for in the sample-and-hold implementation of the control actions, which requires the disturbances $w(t)$ and the sampling period Δ to be sufficiently small such that Eq. (15) is satisfied. However, in the presence of time-varying disturbances that are not sufficiently small as is assumed in the manuscript (i.e., $|w(t)| \leq w_m$ does not hold), the nonlinear system of Eq. (1) may lose closed-loop stability and safety in terms of the boundedness of state in the safe stability region due to a considerable model mismatch between the actual nonlinear process under disturbances and the RNN models that are developed for the nominal system of Eq. (1) with $w(t) \equiv 0$. In this case, real-time adaptive machine-learning-based predictive control can be employed to mitigate the impact of disturbances by updating RNN models online using the most recent process data (Wu et al., 2019b). Specifically, if $x(t_k) \in \mathcal{U}_\rho \backslash \mathcal{U}_{\rho_e}$, we can develop an event-trigger mechanism based on the decreasing rate of CLBF to activate an online update of RNN models when $W_c(x(t)) \leq W_c(x(t_k)) - \epsilon_w(t - t_k)$, $\forall t \in [t_k, t_{k+1})$ is violated, where ϵ_w is obtained in Eq. (12a) as the upper bound for $\dot{W}_c$ accounting for sample-and-hold implementation and sufficiently small disturbances. Additionally, to derive a new ensemble of RNN models when $x(t_k) \in \mathcal{U}_{\rho_e}$, we can utilize an error-trigger mechanism based on the accumulated prediction errors since N_b samplings periods ago (i.e., $E_{rnn}(t_k) = \sum_{i=0}^{N_b} \frac{|x_p(t_{k-i}) - x(t_{k-i})|}{|x(t_{k-i})| + \delta}$, where x_p and x are predicted states and actual state measurements, respectively, and δ is a small positive real number to avoid the division by small numbers).

Table 1 – Parameter values of the CSTR.

$T_0 = 300$ K	$F = 5\,m^3/h$
$V = 1\,m^3$	$E = 5 \times 10^4$ kJ/kmol
$k_0 = 8.46 \times 10^6\,m^3/kmol\,h$	$\Delta H = -1.15 \times 10^4$ kJ/kmol
$C_p = 0.231$ kJ/kg K	$R = 8.314$ kJ/kmol K
$\rho_L = 1000\,kg/m^3$	$C_{A0_s} = 4\,kmol/m^3$
$Q_s = 0.0$ kJ/h	$C_{A_s} = 1.22\,kmol/m^3$
$T_s = 438$ K	

4. Application to a chemical process example

In this section, a chemical process example is utilized to illustrate the application of the proposed CLBF-EMPC scheme that incorporates an ensemble of RNN models for prediction. We consider a well-mixed, non-isothermal continuous stirred tank reactor (CSTR) where an irreversible second-order exothermic reaction takes place. The reaction converts the reactant A to the product B via the chemical reaction $A \rightarrow B$. A heating jacket that supplies or removes heat from the reactor is used. The CSTR dynamic model derived from material and energy balances is given below:

$$\frac{dC_A}{dt} = \frac{F}{V}(C_{A0} - C_A) - k_0 e^{-E/RT} C_A^2 \tag{17a}$$

$$\frac{dT}{dt} = \frac{F}{V}(T_0 - T) + \frac{-\Delta H}{\rho_L C_p} k_0 e^{-E/RT} C_A^2 + \frac{Q}{\rho_L C_p V} \tag{17b}$$

where C_A is the concentration of reactant A in the reactor, V is the volume of the reacting liquid in the reactor, T is the temperature of the reactor and Q denotes the heat input rate. The concentration of reactant A in the feed is C_{A0}. The feed temperature and volumetric flow rate are T_0 and F, respectively. The reacting liquid has a constant density of ρ_L and a heat capacity of C_p. ΔH, k_0, E, and R represent the enthalpy of reaction, pre-exponential constant, activation energy, and ideal gas constant, respectively. Process parameter values are listed in Table 1.

The CSTR is initially operated at the unstable steady-state (C_{As}, T_s) = (1.95 kmol/m^3, 402 K), and (C_{A0_s} Q_s) = (4 kmol/m^3, 0 kJ/h). The manipulated inputs are the inlet concentration of species A and the heat input rate, which are represented by the deviation variables $\Delta C_{A0} = C_{A0} - C_{A0_s}$, $\Delta Q = Q - Q_s$, respectively. The manipulated inputs are bounded as follows: $|\Delta C_{A0}| \leq 3.5\,kmol/m^3$ and $|\Delta Q| \leq 5 \times 10^5$ kJ/h. The states and the inputs of the closed-loop system are $x^T = [C_A - C_{As}\, T - T_s]$ and $u^T = [\Delta C_{A0} \Delta Q]$, respectively, such that the equilibrium point of the system is at the origin of the state-space, (i.e., $(x_s^*, u_s^*) = (0, 0)$).

The explicit Euler method with an integration time step of $h_c = 2 \times 10^{-5}$ h is applied to numerically simulate the dynamic model of Eq. (17). The RNN model is developed in Python using an open-source neural network library, termed Keras. The nonlinear optimization problem of the CLBF-EMPC of Eq. (9) is solved using the python module of the IPOPT software package (Wächter and Biegler, 2006), named PyIpopt with the sampling period $\Delta = 2 \times 10^{-3}$ h. The RNN model is called within the CLBF-EMPC of Eq. (9) each sampling step. Specifically, the RNN model is used in the objective function and the constraints of the CLBF-EMPC optimization problem to predict future states over the prediction horizon giving the state measurement at each sampling step.

4.1. Development of an RNN ensemble

To implement the RNN-based CLBF-EMPC in the closed-loop simulation of the nonlinear system of Eq. (17), we developed an ensemble of RNN models that well approximate the nonlinear dynamics of Eq. (17) in an operating region around the steady-state. Extensive open-loop simulations starting from various initial states in the operating region considered associated with different inputs $u \in U$ are performed to obtain a sufficiently large dataset consisting of state trajectories that can be used for training. The RNN model is constructed with one input layer, two hidden layers consisting of 96 and 64 recurrent units, respectively, and one output layer. The RNN inputs are the initial states x and the input sequences u for each state trajectory, and the RNN outputs are the predicted state trajectory over the simulation period. It is noted that the data points with the time interval of h_c (i.e., the integration time step for the explicit Euler method) are treated as the internal states for RNN models, and will be used during the training process of RNN models. A 10-fold cross-validation is utilized to develop an ensemble of 10 RNN models for the CLBF-EMPC of Eq. (9). Parallel computing is employed to generate 10 RNN models in parallel to speed up the entire training process. Additionally, when implementing the ensemble of RNN models as the prediction model for the CLBF-EMPC of Eq. (9) in the closed-loop simulations below, we also parallelize the computation of multiple RNN models to improve the computational efficiency of real-time implementation of CLBF-EMPC. It is noted that the size of ensemble affects the prediction performance of RNN models and the computational efficiency of closed-loop implementation. In Wu et al. (2019c), we demonstrated that as the number of regression models used in MPC increases, the closed-loop performance was improved in terms of less oscillation. Therefore, the optimal number of RNN models is determined by increasing the number of RNN models in an ensemble until no further improvement is noticed for more RNN models being used. Additionally, as we are using parallel computing to carry out multiple RNN predictions concurrently, the computation time will slightly increase as the number of RNN models increases due to the increasing communication time between the host computing core and other worker cores. Therefore, in this example, 10 RNN models were used to achieve the desired prediction performance and efficient computation simultaneously. The details of developing an ensemble of RNN models for this CSTR example can be found in Wu et al. (2019c).

4.2. Simulation results

The control objective of EMPC is to maximize the profit of the CSTR process of Eq. (17) by manipulating the inlet concentration ΔC_{A0} and the heat input rate ΔQ, while maintaining the closed-loop state trajectories in the safe stability region $\mathcal{U}_\rho$ for all times. The objective function of the CLBF-EMPC is of the following form:

$$l_e(\tilde{x}, u) = k_0 e^{-E/RT} C_A^2 \tag{18}$$

Additionally, a material constraint is incorporated in the CLBF-EMPC of Eq. (9) to make the averaged reactant material available within the entire operating period t_p to be its steady-state value, C_{A0s}. The material constraint is formulated as follows:

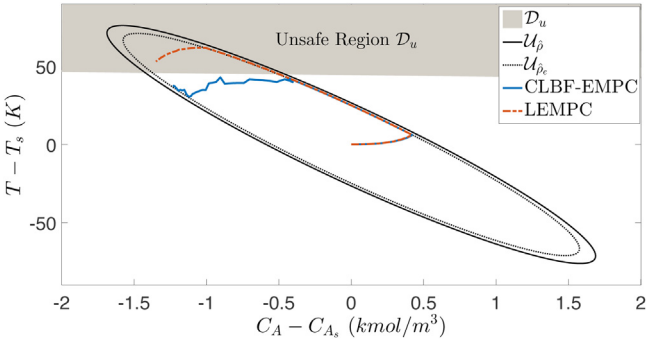

Fig. 1 – Closed-loop state trajectories for the system of Eq. (17) within one operating period under the CLBF-EMPC and the LEMPC, respectively, where the initial condition is (0, 0) and the unbounded set of unsafe states $\mathcal{D}_u$ is the gray area on the top of $\mathcal{U}_\rho$.

$$\frac{1}{t_p}\int_0^{t_p} u_1(\tau)d\tau = 0\,\mathrm{kmol/m^3} \tag{19}$$

where the averaged reactant material in deviation form, u_1, is equal to 0. We first demonstrate the application of the proposed CLBF-EMPC control scheme to an unbounded unsafe region $\mathcal{D}_u$ in state-space. The unsafe region is characterized as an unbounded set with high temperature and concentration for the CSTR of Eq. (17): $\mathcal{D}_u := \{x \in \mathbf{R}^2 | F(x) = x_1 + x_2 > 47\}$, where the threshold is set to be 47. As the objective of EMPC is to dynamically optimize the profit of the CSTR process of Eq. (17) by maximizing the production rate $r = k_0 e^{-E/RT} C_A^2$, it is observed in Fig. 1 that under the Lyapunov-based EMPC of Eq. (8) that does not account for safety issue, the closed-loop state is driven to the top of the operating region where temperature is much higher than the steady-state value, to obtain an increased economic profits compared to the steady-state operation (i.e., the system is operated at steady-state for all times). Additionally, by designing the unbounded unsafe region with the form of $F(x) = x_1 + x_2$, it is noted that the temperature in the reactor plays a more important role in characterizing the unsafe region $\mathcal{D}_u$ than the concentration due to its larger magnitude. This is consistent with the operation of an exothermic reaction in CSTR, where rapid increases in temperature might lead to potential safety problems. However, it should be mentioned that reactant concentration is still accounted for in the characterization of the unbounded unsafe region $\mathcal{D}_u$ due to its impact on the reaction rate.

Following the construction method of a CLBF in Wu et al. (2019a), we design a Control Lyapunov function with the standard quadratic form $V(x) = x^T P x$, where $P = \begin{bmatrix} 1060 & 22 \\ 22 & 0.52 \end{bmatrix}$. The matrix P in CLF is determined by trial-and-error to maximize the stability region (i.e., the largest level set of Lyapunov function V in the region where the time-derivative of V can be rendered negative under the Lyapunov-based controller). Additionally, the CLF can also be constructed using the construction method for a constrained CLF in Mahmood and Mhaskar (2014), Homer and Mhaskar (2017). Then, we characterize a set $\mathcal{H}$ that contains $\mathcal{D}_u$: $\mathcal{H} := \{x \in \mathbf{R}^2 | F(x) > 45\}$, and design the control barrier function $B(x)$ as follows:

$$B(x) = \begin{cases} e^{F(x)-47} - 2 \times e^{-2}, & \text{if } x \in \mathcal{H} \\ -e^{-2}, & \text{if } x \notin \mathcal{H} \end{cases} \tag{20}$$

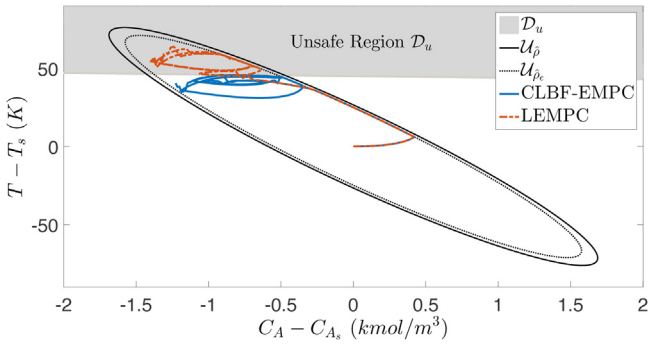

Fig. 2 – Closed-loop state trajectories for the system of Eq. (17) within four operating periods under the CLBF-EMPC and the LEMPC, respectively, where the initial condition is (0, 0) and the unbounded set of unsafe states $\mathcal{D}_u$ is the gray area on the top of $\mathcal{U}_\rho$.

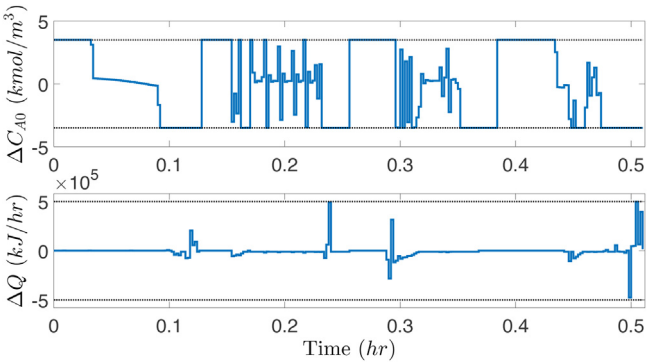

Fig. 3 – Input profiles for the closed-loop system of Eq. (17) within four operating periods under CLBF-EMPC, where the unsafe region is the gray area on the top of $\mathcal{U}_\rho$.

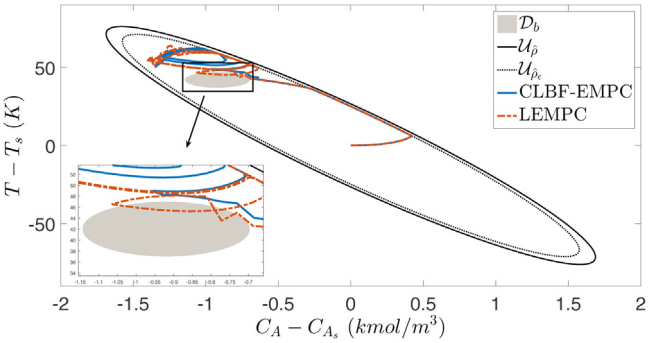

Fig. 4 – Closed-loop state trajectories for the system of Eq. (17) within four operating periods under the CLBF-EMPC and the LEMPC, respectively, where the initial condition is (0, 0) and the bounded set of unsafe states $\mathcal{D}_b$ is embedded within $\mathcal{U}_\rho$.

The control Lyapunov-barrier function $W_c(x) = V(x) + \mu B(x) + \nu$ is constructed with the following parameters: $\rho = 0$, $c_1 = 0.1$, $c_2 = 1061$, $c_3 = 5808$, $c_4 = 2259$, $\nu = \rho - c_1 c_4 = -225.9$, and $\mu = 4.6 \times 10^7$. The definitions of the above parameters can be found in Wu et al. (2019a).

The closed-loop simulation results for the system of Eq. (17) under the RNN-based CLBF-EMPC of Eq. (9), and the LEMPC of Eq. (8) are shown in Figs. 1–3 . Specifically, Fig. 1 shows the comparison of the state trajectories under LEMPC and CLBF-EMPC, respectively. It is demonstrated that starting from the initial condition (0, 0), the state trajectory for one simulation period $t_p = 0.128$ h under CLBF-EMPC is maintained below the unbounded unsafe region $\mathcal{D}_u$ for all times, while the one under LEMPC exceeds the threshold and enters $\mathcal{D}_u$ near the end of simulation.

In the second simulation, we run the closed-loop simulation for successive four operating period, where each operating period is $t_p = 0.128$ h. The material constraint is imposed in each operating period such that the averaged reactant material (in deviation form) within each operating period equals zero. It is demonstrated in Fig. 2 that the state trajectory under the CLBF-EMPC of Eq. (9) remains in the safe stability region $\mathcal{U}_\rho$ within four operating periods, while the one under LEMPC enters the unsafe region during the first operating period and stays there for the remainder of the process operation. Both state trajectories progress in a circular manner in the stability region (the solid ellipse) because the material constraint forces the decrease of the reactant concentration near the end of each operating period. This can also be observed in the input profiles for the closed-loop system of Eq. (17) within four operating periods shown in Fig. 3, where CLBF-EMPC consumes the maximum allowable ΔC_{A0} at the beginning of each operating period and lowers the consumption near the end.

In addition, we calculate the total economic profits over four operating periods, i.e., $L_E = \int_{t=0}^{4t_p} k_0 e^{-E/RT} C_A^2 dt$, for the closed-loop system of Eq. (17) under the different controllers. It was obtained that the L_E values are 8.42, 8.01 and 5.24 for the closed-loop CSTR under LEMPC, CLBF-EMPC, and steady-state operation, respectively, from which it is demonstrated that economic profits are significantly improved (around 52%) under EMPC compared to the steady-state operation. The reason for a slightly larger L_E under LEMPC than CLBF-EMPC is that the state under LEMPC enters the unsafe region during the simulation where increased production rate is obtained due to higher temperature (Fig. 2).

The second example is to demonstrate the effectiveness of the CLBF-EMPC of Eq. (9) for the system with a bounded unsafe region $\mathcal{D}_b$ in state-space. The bounded unsafe region $\mathcal{D}_b$ is designed to be a set embedded within the stability region as shown in the above example to demonstrate that the CLBF-EMPC of Eq. (9) is able to achieve economic optimality while maintaining the state out of $\mathcal{D}_b$ for all times. The unsafe region is developed as an ellipse: $\mathcal{D}_b := \{x \in \mathbf{R}^2 | F(x) = \frac{(x_1+0.92)^2}{1} + \frac{(x_2-42)^2}{500} < 0.06\}$. $\mathcal{H}$ is defined as $\mathcal{H} := \{x \in \mathbf{R}^2 | F(x) < 0.07\}$. The control barrier function $B(x)$ is defined as follows:

$$B(x) = \begin{cases} e^{\frac{F(x)}{F(x) - 0.07}} - e^{-6}, & \text{if } x \in \mathcal{H} \\ -e^{-6}, & \text{if } x \notin \mathcal{H} \end{cases} \tag{21}$$

The control Lyapunov-barrier function $W_c(x) = V(x) + \mu B(x) + \nu$ is developed following the same construction method as in the first example with the following parameters: $c_1 = 0.1$, $c_2 = 1061$, $c_3 = \max_{x \in \partial\mathcal{H}} |x|^2 = 2295$, $c_4 = \min_{x \in \partial\mathcal{D}} |x|^2 = 1370$, $\nu = \rho_c - c_1 c_4 = -160$, and $\mu = 1 \times 10^9$. Since there exist stationary point in state-space in the case of a bounded unsafe region, we let $\frac{\partial W_c(x)}{\partial x} = 0$ and obtain the stationary point of $W_c(x)$ (for $x \neq 0$) as $x_e = (-1.004, 47.48)$. Therefore, $\mathcal{U}_{\rho_e}$ should be designed to include this point inside such that it does not affect closed-loop stability under CLBF-EMPC.

The simulation results for the closed-loop system of Eq. (17) under CLBF-EMPC are shown in Figs. 4 and 5 . Specifically, in Fig. 4, it is demonstrated that the state trajectory

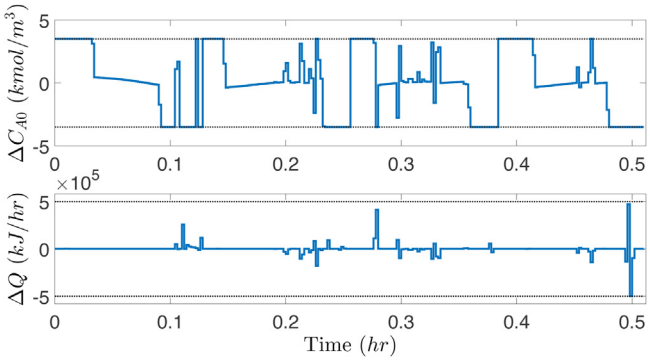

Fig. 5 – Input profiles for the closed-loop system of Eq. (17) within four operating periods under CLBF-EMPC, where the bounded set of unsafe states $\mathcal{D}_b$ is embedded within $\mathcal{U}_\rho$.

under CLBF-EMPC is maintained in the safe stability region $\mathcal{U}_\rho$ for all times (i.e., four successive operating periods with $t_p = 0.128$ h). However, the state trajectory under LEMPC enters the bounded unsafe region $\mathcal{D}_b$ since the design of the LEMPC of Eq. (8) does not account for any safety constraints. Similarly, Fig. 5 shows the input profiles for the closed-loop system of Eq. (17) within four operating periods under the CLBF-EMPC of Eq. (9), where ΔC_{A0} shows variation due to the material constraint of Eq. (19) applied in each operating period. Additionally, the accumulated economic profits are calculated for the closed-loop system of Eq. (17) in the presence of a bounded unsafe region. It was found that the L_E values are 8.42, 8.47 and 5.24 for LEMPC, CLBF-EMPC, and steady-state operation, respectively. This again demonstrates that process economics is optimized under EMPC while closed-loop stability and process operational safety are both guaranteed. It is noted that the total economic profits under LEMPC and under CLBF-EMPC are very close since the two state trajectories both stay in a region above the unsafe set for most of the process operation time (Fig. 4). The only difference is that the state trajectory under CLBF-EMPC avoids the bounded unsafe region for all times, while the one under LEMPC does not.

Additionally, it is noted that the RNN-based MPC is computationally more demanding than the first-principles-model-based MPC because the RNN model is essentially a complicated nonlinear function which requires more computation time for prediction. In our example, the computation time for running RNN-based MPC is around 2.3 s, which is less than one sampling period (i.e., 2×10^{-3} h = 7.2 s) such that it can be implemented in real-time optimization and control. The above case studies demonstrate that the CLBF-EMPC of Eq. (9) based on an ensemble of RNN models achieved desired model prediction results for the nonlinear system of Eq. (17), and thus, is able to optimize control actions that maintain the closed-loop state within the safe stability region $\mathcal{U}_\rho$ for all times. Additionally, we demonstrate the applicability of the CLBF-EMPC of Eq. (9) to both bounded and unbounded unsafe regions in a CSTR example. The economic profits over multiple operating periods are calculated and compared under LEMPC, CLBF-EMPC and steady-state operation, respectively, from which it can be concluded that significant improvement of economic benefits can be achieved under EMPC.

5. Conclusion

In this work, we proposed an RNN-based CLBF-EMPC system that can be utilized to operate the nonlinear process in a time-varying manner to achieve economic optimality with guaranteed closed-loop stability and process operational safety. Under the condition that an accurate process model (i.e., the first-principles model) is not available, an ensemble of RNN models was developed to approximate the dynamic behavior of nonlinear processes using process data in an operating region. The RNN-based CLBF-EMPC that utilizes an ensemble of RNN models for prediction, and CLBF-based constraints to ensure boundedness of the state in the safe stability region was designed for nonlinear processes with bounded and unbounded unsafe regions. The effectiveness of the proposed RNN-based CLBF-EMPC method was demonstrated through an application to a chemical process example, within which simultaneous economic optimality and operational safety were achieved for two types (bounded and unbounded) of unsafe regions.

Conflict of interest

None declared.

Acknowledgments

Financial support from the National Science Foundation and the Department of Energy is gratefully acknowledged.

References

Ali, J.M., Hussain, M.A., Tade, M.O., Zhang, J., 2015. Artificial intelligence techniques applied as estimator in chemical process systems – a literature survey. Expert Syst. Appl. 42, 5915–5931.

Ames, A.D., Coogan, S., Egerstedt, M., Notomista, G., Sreenath, K., Tabuada, P., 2019. Control Barrier Functions: Theory and Applications. arXiv:1903.11199.

Ames, A.D., Grizzle, J.W., Tabuada, P., 2014. Control barrier function based quadratic programs with application to adaptive cruise control. In: Proceedings of the 53rd IEEE Conference on Decision and Control, Los Angeles, CA, pp. 6271–6278.

Angeli, D., Amrit, R., Rawlings, J.B., 2012. On average performance and stability of economic model predictive control. IEEE Trans. Autom. Control 57, 1615–1626.

Braun, P., Kellett, C.M., 2018. On (The Existence Of) Control Lyapunov Barrier Functions, Preprint, https://eref.uni-bayreuth.de/40899.

Ellis, M., Durand, H., Christofides, P.D., 2014. A tutorial review of economic model predictive control methods. J. Process Control 24, 1156–1178.

Heidarinejad, M., Liu, J., Christofides, P.D., 2013. Economic model predictive control of switched nonlinear systems. Syst. Control Lett. 62, 77–84.

Homer, T., Mhaskar, P., 2017. Constrained control Lyapunov function-based control of nonlinear systems. Syst. Control Lett. 110, 55–61.

Jankovic, M., 2017. Combining control Lyapunov and barrier functions for constrained stabilization of nonlinear systems. In: Proceedings of the American Control Conference, Seattle, WA, pp. 1916–1922.

Kosmatopoulos, E.B., Polycarpou, M.M., Christodoulou, M.A., Ioannou, P.A., 1995. High-order neural network structures for identification of dynamical systems. IEEE Trans. Neural Netw. 6, 422–431.

Leveson, N.G., Stephanopoulos, G., 2014. A system-theoretic, control-inspired view and approach to process safety. AIChE J. 60, 2–14.

Lin, Y., Sontag, E.D., 1991. A universal formula for stabilization with bounded controls. Syst. Control Lett. 16, 393–397.

Mahmood, M., Mhaskar, P., 2014. Constrained control Lyapunov function based model predictive control design. Int. J. Robust Nonlinear Control 24, 374–388.
Malisoff, M., Mazenc, F., 2009. Constructions of Strict Lyapunov Functions. Springer Science & Business Media.
Mannan, M.S., Sachdeva, S., Chen, H., Reyes-Valdes, O., Liu, Y., Laboureur, D.M., 2015. Trends and challenges in process safety. AIChE J. 61, 3558–3569.
Mehra, A., Ma, W., Berg, F., Tabuada, P., Grizzle, J.W., Ames, A.D., 2015. Adaptive cruise control: experimental validation of advanced controllers on scale-model cars. In: Proceedings of the American Control Conference, Chicago, IL, pp. 1411–1418.
Müller, M.A., Angeli, D., Allgöwer, F., 2013. Economic model predictive control with self-tuning terminal cost. Eur. J. Control 19, 408–416.
Niu, B., Zhao, J., 2013. Barrier Lyapunov functions for the output tracking control of constrained nonlinear switched systems. Syst. Control Lett. 62, 963–971.
Romdlony, M.Z., Jayawardhana, B., 2016. Stabilization with guaranteed safety using control Lyapunov-barrier function. Automatica 66, 39–47.
Sanders, R.E., 2015. Chemical Process Safety: Learning From Case Histories. Butterworth-Heinemann.
Smith, H., Howard, C., Foord, T., 2003. Alarms management/priority, floods, tears or gain? introduction to the “problem”. Meas. Control 36, 109–113.
Sontag, E.D., 1989. A ‘universal’ construction of Artstein’s theorem on nonlinear stabilization. Syst. Control Lett. 13, 117–123.
Tee, K.P., Ge, S.S., Tay, E.H., 2009. Barrier Lyapunov functions for the control of output-constrained nonlinear systems. Automatica 45, 918–927.
Venkatasubramanian, V., 2011. Systemic failures: challenges and opportunities in risk management in complex systems. AIChE J. 57, 2–9.
Wächter, A., Biegler, L.T., 2006. On the implementation of an interior-point filter line-search algorithm for large-scale nonlinear programming. Math. Program. 106, 25–57.
Wieland, P., Allgöwer, F., 2007. Constructive safety using control barrier functions. IFAC Proc. 40, 462–467.
Wong, W., Chee, E., Li, J., Wang, X., 2018. Recurrent neural network-based model predictive control for continuous pharmaceutical manufacturing. Mathematics 6, 242.
Wu, Z., Albalawi, F., Zhang, Z., Zhang, J., Durand, H., Christofides, P.D., 2019a. Control Lyapunov-barrier function-based model predictive control of nonlinear systems. Automatica 109, 108508.
Wu, Z., Christofides, P.D., 2019. Handling bounded and unbounded unsafe sets in control Lyapunov-barrier function-based model predictive control of nonlinear processes. Chem. Eng. Res. Des. 143, 140–149.
Wu, Z., Rincon, D., Christofides, P.D., 2019b. Real-time adaptive machine-learning-based predictive control of nonlinear processes. Ind. Eng. Chem. Res., http://dx.doi.org/10.1021/acs.iecr.9b03055.
Wu, Z., Tran, A., Rincon, D., Christofides, P.D., 2019c. Machine learning-based predictive control of nonlinear processes. Part I. Theory. AIChE J. 65, e16729.